

# Design of a Multitask Reactive Distillation with Intermediate Heat Exchangers for the Production of Silane and Chlorosilane Derivates

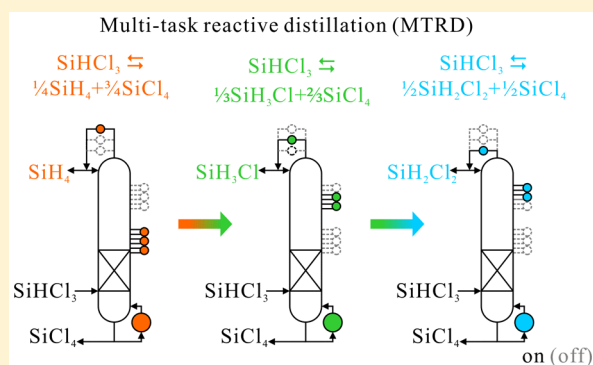
J. Rafael Alcántara-Avila,<sup>\*,†</sup> Morihiro Tanaka,<sup>†</sup> César Ramírez Márquez,<sup>‡</sup> Fernando I. Gómez-Castro,<sup>‡</sup> J. Gabriel Segovia-Hernández,<sup>‡</sup> Ken-Ichiro Sotowa,<sup>†</sup> and Toshihide Horikawa<sup>†</sup>

<sup>†</sup>Department of Applied Chemistry, Graduate School of Science and Technology, Tokushima University, 2-1 minami Josanjima-cho, Tokushima 770-8506, Japan

<sup>‡</sup>Departamento de Ingeniería Química, Universidad de Guanajuato, Noria Alta s/n, Guanajuato 36050, Mexico

## Supporting Information

**ABSTRACT:** Silane and chlorosilanes are essential materials for manufacturing silicon solar cells, glass microscope slides, oxidation masks, and corrosion-resistant films among other products. Monochlorosilane ( $\text{SiH}_3\text{Cl}$ ) and dichlorosilane ( $\text{SiH}_2\text{Cl}_2$ ) are produced on a large scale as intermediates in the synthesis of silane ( $\text{SiH}_4$ ) by disproportionation of trichlorosilane ( $\text{SiHCl}_3$ ). However, seldom are they isolated due to the highly integrated nature of silane production, and the high commercial demand for silane relative to monochlorosilane and dichlorosilane. This study proposes a multitask reactive distillation (MTRD) column with intermediate heat exchangers that has the flexibility to switch between the production of  $\text{SiH}_4$ ,  $\text{SiH}_3\text{Cl}$ , and  $\text{SiH}_2\text{Cl}_2$  from the  $\text{SiHCl}_3$  disproportionation. Because the reactive distillation that separates  $\text{SiH}_4$  uses an expensive refrigerant, intermediate heat exchangers are installed to reduce the cost and energy consumption of expensive refrigerants in the optimized MTRD. Process simulation and mathematical programming optimization tools are combined to find the best number, location, and heat distribution of intermediate exchangers.



## 1. INTRODUCTION

Silane and chlorosilanes are the essential chemicals for the production of silicon-based solar cells, microscopic glass slides, oxidation masks, and corrosion-resistant coating. They are used in a wide variety of innovative applications.

More than 90% of all solar cells use silicon in various crystalline or amorphous structural forms. Bye and Ceccaroli<sup>1</sup> presented a thorough review and comparison regarding energy consumption, product quality, and technology cost among the Siemens process, the fluidized bed reactor process, and the upgraded metallurgical grade silicon process, which are the major technologies that dominate the photovoltaic industry. The Siemens process is the dominant technology. It produces trichlorosilane (TCS) from metallurgical grade silicon (MGS), purifies it through several distillation and condensation steps, and decomposes it in a thermal chemical vapor deposition (CVD) reactor. The fluidized bed reactor (FBR) process uses silane ( $\text{SiH}_4$ ). This process attains an important reduction of the energy consumed in the deposition process. Silane gas can be completely converted to elementary silicon with hydrogen gas as the only byproduct. Finally, the upgraded metallurgical grade (UMG) silicon process uses metallurgical routes to remove impurities (e.g., transition elements, carbon) from silicon. However, silicon still has a high dopant level, which

limits its application. Figure 1 summarizes a variety of routes to produce solar grade silicon (SGS) from silicon dioxide ( $\text{SiO}_2$ ).<sup>2</sup>

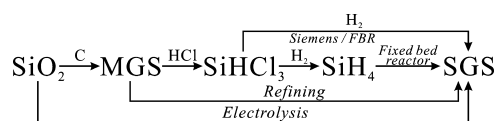


Figure 1. Routes to produce solar grade silicon.

Silanes with low chlorine content are desirable precursors for the production of functionalized silanes containing the  $\text{SiH}_3^+$  or  $\text{SiH}_2^{+2}$  functional groups. The properties of the functionalized silanes have proven to be highly tunable by variation of their substituents and have found a wide variety of industrial, biological, or environmental applications.<sup>3</sup>

Aminosilane ( $\text{SiH}_3\text{NH}_2$ ) can be generated by reacting monochlorosilane ( $\text{SiH}_3\text{Cl}$ ) with the amino radical ( $\text{NH}_2^\cdot$ ). The nucleophilicity of  $\text{NH}_2$  groups in amino silanes is useful to promote adhesion in glass-resin composites. In aqueous media,

Received: June 12, 2016

Revised: August 30, 2016

Accepted: September 9, 2016

Published: September 9, 2016

NH<sub>3</sub><sup>+</sup> groups promote the attachment of negatively charged species, such as DNA and nanoparticles.<sup>4</sup>

Silicon nitride (Si<sub>3</sub>N<sub>4</sub>) can be generated by reacting dichlorosilane (SiH<sub>2</sub>Cl<sub>2</sub>) and ammonia (NH<sub>3</sub>), and it is a material of high technological importance because of its electronic and optical properties (i.e., high dielectric constant and large band gap), mechanical strength and hardness, and exceptional thermal and chemical stability.<sup>5</sup>

Although monochlorosilane and dichlorosilane are produced on a large scale as intermediates in the industrial synthesis of silane by disproportionation of trichlorosilane, seldom are they isolated due to the highly integrated nature of silane production, and the high commercial demand for silane relative to monochlorosilane and dichlorosilane.

The conventional silane manufacturing process has three reactors and two distillation columns.<sup>6</sup> Owing to unfavorable chemical equilibrium, the disproportionation reaction of trichlorosilane (SiHCl<sub>3</sub>) and the separation of SiH<sub>4</sub> requires a very large recycle ratio, which results in high energy consumption as well as capital investment. Therefore, reactive distillation (RD), which is a technology that combines reaction and distillation in one column, is particularly attractive for equilibrium limited reactions, and the conventional silane manufacturing process can be summarized in a reactive distillation,<sup>7,8</sup> or a series of two reactive distillation columns.<sup>9</sup>

The separation of multicomponent mixtures in reactive distillation has been researched mostly for batch processes because a batch still can be very flexible to accommodate different multicomponent batch charges and to allow the collection over time of a series of product cuts of different compositions.<sup>10</sup> However, the separation of multicomponent mixtures involving chemical reactions has drawn less attention. Kapilakam and Luyben<sup>11</sup> addressed a hypothetical system having a single reactor in which three reactions produce three components, and having three distillation columns to remove each desired component. The desired production rate of each component was met by adjusting the ratio of the fresh feeds, and the two recycle flow rates. A more recent work addressed the design and control of a system having a reactor and a distillation column to manufacture furfuryl alcohol and 2-methylfuran simultaneously in which distribution switching between products was possible.<sup>12</sup>

This work does not simultaneously produce silane, monochlorosilane, and dichlorosilane, but exclusively one of them in any desired sequential order. Thus, the proposed system is not a multiproduct reactive distillation (MPRD), but a multitask reactive distillation (MTRD).

It is of great importance to produce silane and its derivatives reliably and safely especially when the reflux ratio, reboiler duty, and top pressure must be manipulated for online switching between products. Ramírez-Márquez et al.<sup>13</sup> have studied the process control of an MTRD without intermediate heat exchangers that produces silane, monochlorosilane, and dichlorosilane at a fixed pressure. The authors show that dual point temperature control suffices to keep the purity of each product at 99.5 mol %. Also, their results show that a gradual variation of the feed-to-distillate ratio and reboiler duty can switch online the production between dichlorosilane–monochlorosilane–silane–monochlorosilane–dichlorosilane within 60 h where the dichlorosilane–monochlorosilane–dichlorosilane switch was the fastest (less than 10 h).

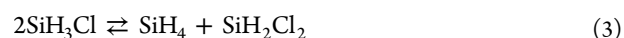
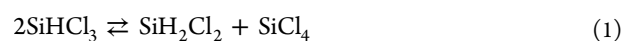
The motivation of this work focuses on the use of intermediate condensers and reboilers to lower the energy

consumption and cost of expensive refrigerants. One of the major disadvantages in using reactive distillation for the disproportionation of trichlorosilane is the low boiling point of silane at the top of the column, which is around –112 °C. Therefore, the use of intermediate condensers has been proposed to reduce the energy consumption and cost of the refrigeration load at the top of the column.<sup>7,8</sup>

The approach presented in this work is a straightforward extension of our previous work<sup>8</sup> to the design of an MTRD with intermediate heat exchangers and with a broader choice of utilities and refrigeration cycles. The proposed reactive distillation system has the flexibility to switch the production of silane, monochlorosilane, and dichlorosilane by changing the operation variables (e.g., reflux ratio, reboiler duty, the amount of heat transfer in intermediate condensers and reboilers) and structural variables (e.g., number and location of intermediate condensers and reboilers).

## 2. KINETIC AND THERMODYNAMIC MODELS

There are at least three commercial processes to make silane.<sup>1</sup> From the possible methods to produce silane; this work adopts the disproportionation of purified trichlorosilane because monochlorosilane and dichlorosilane are also generated in the reaction system. The reactions in eqs 1 to 3 take place in the liquid phase by using the resin Amberlyst A-21 as a catalyst.



The pseudohomogeneous second order kinetic expressions<sup>7,8</sup> for eqs 1 to 3 are shown in eqs 4 to 6.

$$r_1 = k_{1,i} e^{(-E_1/RT)} \left( x_{\text{TCS}}^2 - \frac{x_{\text{DCS}} x_{\text{STC}}}{K_1 e^{(-\Delta H_1/RT)}} \right) \quad (4)$$

$$r_2 = k_{2,i} e^{(-E_2/RT)} \left( x_{\text{DCS}}^2 - \frac{x_{\text{MCS}} x_{\text{TCS}}}{K_2 e^{(-\Delta H_2/RT)}} \right) \quad (5)$$

$$r_3 = k_{3,i} e^{(-E_3/RT)} \left( x_{\text{MCS}}^2 - \frac{x_{\text{S}} x_{\text{DCS}}}{K_3 e^{(-\Delta H_3/RT)}} \right) \quad (6)$$

where  $r$  denotes the reaction rate,  $k_i$  and  $K_i$  are pre-exponential factors for the kinetic constant and the equilibrium constant, respectively.  $E_i$  is the activation energy of the forward reaction, and  $\Delta H_i$  is the heat of reaction for all  $i = 1, \dots, 3$ . S, MCS, DCS, TCS, STC are the subscripts that represent silane, monochlorosilane, dichlorosilane, trichlorosilane, and silicon tetrachloride, respectively. Finally,  $x_i$  denotes the mole fraction of the component  $i$ .

Table 1 summarizes the values in eqs 4 to 6. They were regressed from experimental data and taken from Huang et al.<sup>7</sup>

**Table 1.** Kinetic Parameters for the Disproportionation of Trichlorosilane

$r_i$	$k_{0,i}$ [1/s]	$K_{0,i}$ [–]	$E_i$ [J/mol]	$\Delta H_i$ [J/mol]
$r_1$	73.5	0.1856	30045	6402
$r_2$	949466.4	0.7669	51083	2226
$r_3$	1176.9	0.6890	26320	–2548

The atmospheric boiling point of each component is very different between silane  $-112.15\text{ }^{\circ}\text{C}$  and the other components ( $-30\text{ }^{\circ}\text{C}$  for MCS,  $8.3\text{ }^{\circ}\text{C}$  for DCS,  $31.85\text{ }^{\circ}\text{C}$  for TCS, and  $56.85\text{ }^{\circ}\text{C}$  for STC). Thus, the relative volatility between adjacent components is very different. MCS, DCS, and TCS can be maintained in the reaction zone because they have intermediate boiling points. In this work, the Peng–Robinson equation of state was selected to perform thermodynamic vapor–liquid equilibrium calculations. Table 2 shows the adopted binary interaction coefficients  $k_{ij}$  from Huang et al.<sup>7</sup> There are no azeotropes in the reaction system.

**Table 2. Binary Interaction Parameters**

<i>i</i>	<i>j</i>	$k_{ij}$ [–]
SiCl <sub>4</sub>	SiHCl <sub>3</sub>	0.01603
SiCl <sub>4</sub>	SiH <sub>2</sub> Cl <sub>2</sub>	0.02108
SiHCl <sub>3</sub>	SiH <sub>2</sub> Cl <sub>2</sub>	0.05183
SiH <sub>2</sub> Cl <sub>2</sub>	SiH <sub>3</sub> Cl	–0.00538
SiH <sub>3</sub> Cl	SiH <sub>4</sub>	0.000953

### 3. SIMULATION PROCEDURE

The RadFrac module in Aspen Plus 8.6 was used to perform the simulations at steady state. This section explains how the simulations were done to design the reactive distillation column and the refrigeration cycles that provide cooling at the column top condenser and intermediate condensers to produce silane and its derivatives.

**3.1. Simulation of Reactive Distillation Columns.** The equilibrium-based method was used in the RadFrac module, and it solves a system of nonlinear equations that contains material balance, heat balance components, summation equations, and the vapor–liquid equilibrium relations and reaction kinetics described in section 2.

There are several proposed methodologies to design RD columns, which are based on experimental and theoretical calculations.<sup>14–16</sup> The design of RD columns consists in finding structural parameters (e.g., the number of stages, the location of reactive stages, the location of feed stage(s)) and operational parameters (e.g., reflux ratio, reboiler duty, product purity) that minimize any objective function(s). The design of the RD in this study is based on sensitivity analysis through a modular simulator, as described next: (1) Take the original RD design from Huang et al.<sup>7</sup> (2) Perform a sensitivity analysis for the design in step 1. From this design, sensitivity analyses were done by varying the number of stages, number of reactive stages, the feed stage, operating pressure, reflux ratio and stage holdup so as to minimize the reboiler duty of each column simulated independently and the column that can produce silane, monochlorosilane, and dichlorosilane.<sup>13</sup> Table S1 in the Supporting Information summarizes the design parameters of each distillation column that is simulated independently and those of the MTRD.

Figure 5a shows the base case MTRD. One of the most important parameters was the number of stages (NS), which was 65, to ensure 99.5% mol purity of each product. The selected holdup was  $0.15\text{ m}^3$  because it corresponded to the slowest reaction (i.e., monochlorosilane generation).

The operating pressure, the location of reactive stages, and the composition profile in RD play an important role to avoid catalyst thermal resistance deactivation and to achieve the maximum reactant conversion and reaction heat. In this study,

the selected catalyst was the polymeric resin Amberlyst A-21. It is a weakly basic anion exchange resin developed for the removal of acidic materials.<sup>17</sup> Also, the maximum suggested operating temperature is  $100\text{ }^{\circ}\text{C}$  and the minimum bed depth is 0.6 m.

Table 3 summarizes the simulation conditions for the MTRD in this study.

**Table 3. Simulation Conditions for the Reactive Distillation Columns**

Feed	
flow rate [kmol/h]	10
feed mol fraction [%]	100 (TCS)
pressure [bar]	5.07
temperature [ $^{\circ}\text{C}$ ]	50
Products	
S mol fraction [%]	99.5
MCS mol fraction [%]	99.5
DCS mol fraction [%]	99.5
STC mol fraction [%]	$\geq 99.9$
Additional Data	
holdup per stage [ $\text{m}^3$ ]	0.15
pressure drop per stage [bar]	0.005

Figures S1 and S2 in the Supporting Information show the temperature and composition profiles, respectively, for the MTRD that operates at 2.5 bar. In all cases, the reactive section from stage 21 to 50 is under  $100\text{ }^{\circ}\text{C}$ , and the top distillate purity is 99.5 mol %.

Table 4 shows the simulation results from the design parameters in Table S1 in the Supporting Information.

**Table 4. Simulation Results for the MPRD and MTRD Processes**

variable [units]	MPRD			MTRD
	SiH <sub>4</sub>	SiH <sub>3</sub> Cl	SiH <sub>2</sub> Cl <sub>2</sub>	SiH <sub>4</sub> /SiH <sub>3</sub> Cl/ SiH <sub>2</sub> Cl <sub>2</sub>
stages [–]	62	63	65	65
distillate flow rate [kmol/h]	2.5	3.335	5.0	2.5/3.335/5
reflux ratio	77.27	44.32	24.49	61.01/47.49/50.98
condenser duty [kW]	–636.03	–822.83	–821.29	–537.24/–854.37/–1585.45
reboiler duty [kW]	677.50	845.74	832.60	569.70/882.19/ 1606.11

The table shows the MPRD in which each column produces independently silane, monochlorosilane, and dichlorosilane and the conventional MTRD without intermediate heat exchanger in which one column can produce either silane, monochlorosilane, or dichlorosilane.

**3.2. Simulation of Refrigeration Cycles.** A variety of refrigerants is available to provide cooling at the top condenser and intermediate condensers in the rectifying section. Figure 2a shows a conceptual representation of the simulated single stage refrigeration cycle for the refrigerants in Table S2 in the Supporting Information. N<sub>2</sub> was also simulated as the two-stage refrigeration cycle shown in Figure 2b because this arrangement is better to achieve refrigeration at very low temperature (Table S3 in the Supporting Information).<sup>18</sup> The assumed electricity cost in Japan was  $0.188\text{ } \$/\text{kWh}$ .<sup>19</sup>

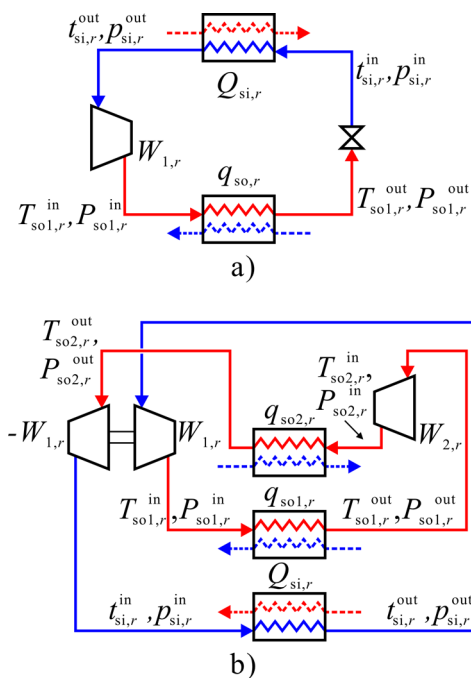


**Figure 2.** Refrigeration cycles: (a) single stage cycle, (b) two-stage cycle.

Section S2 in the [Supporting Information](#) covers in detail the design of refrigeration cycles and its refrigeration cost.

#### 4. OPTIMIZATION OF REACTIVE DISTILLATION WITH INTERMEDIATE HEAT EXCHANGERS

The use of intermediate condensers is beneficial to reduce the consumption of expensive refrigerant at the column top condenser, and in a similar way, the use of intermediate reboilers can be useful to reduce the consumption of expensive steam. Previous results showed that 97% reduction of the refrigeration load at the top condenser can be attained while keeping more than 99 mol % of silane.<sup>7</sup> Consequently, the use of less expensive refrigerant results in less operation cost for the RD. One of our previous works showed that the total cost of the RD for the disproportionation of trichlorosilane is mostly dominated by the cost of cooling and heating utilities. Also, the use of intermediate condensers attained 59% reduction of the operation cost and 56% the reduction of the total annual cost.<sup>8</sup> In this work, the use of intermediate condensers or reboilers is extended to the production of MCS and DCS.

**4.1. Mathematical Model.** [Figure 3](#) shows a reactive distillation column subject to the installation of intermediate heat exchangers. In the figure, S, MCS, or DCS can be produced at the top of the column. The dotted lines represent the heat exchange possibilities between the stages in the rectifying section and heat sinks of the refrigeration cycles, cooling water (CW), and chilled water (CHW). Similarly, the dotted lines represent the heat exchange possibilities between the stages in the stripping section and heat sources of the refrigeration cycles and steam.

Changes in the operation variables can shift the production between S, MCS, and DCS.<sup>13</sup> This section shows the objective function, the most significant constraints, and the solution procedure briefly. For more details about the mathematical formulation and solution procedure, please refer to our previous work.<sup>8</sup>

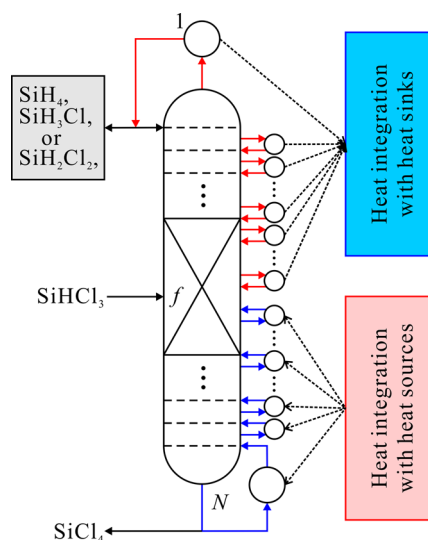


**Figure 3.** Simplified superstructure representation of the heat exchange network between stages and utilities.

[Equation 7](#) shows the minimization of the operating cost because the trichlorosilane disproportionation is mostly dominated by this cost, which can be confirmed by the results in [section 5](#),

$$OC = \sum_{p \in \text{PRO}} \theta_p \left( \sum_{\substack{i \in \text{REC} \\ j \in \text{CU}}} Q_{p,i,j}^{\text{ex}} C_j^{\text{cool}} + \sum_{\substack{i \in \text{HU} \\ j \in \text{STR}}} Q_{p,i,j}^{\text{ex}} C_i^{\text{heat}} \right) \quad (7)$$

where PRO is the set of products leaving the reactive distillation column at the top, REC and STR are the sets of stages in the rectifying and stripping sections, and CU and HU are the sets of cooling and heating utilities, respectively.  $\theta_p$  is the number of annual operation hours designated for each product.  $Q_{p,i,j}^{\text{ex}}$  is the amount of heat exchanged between a heat source  $i$  and a heat sink  $j$  for each product  $p$ .  $C_j^{\text{cool}}$  and  $C_i^{\text{heat}}$  is the cooling and heating cost, respectively.

The following equations show the most relevant constraints in the optimization problem. [Equations 8](#) and [9](#) show the energy balance in the heat exchange network between stages and utilities

$$Q_p^{\text{cn}} = Q_{0,p}^{\text{cn}} - \sum_{i \in \text{REC}'} (\Delta Q_{p,i}^{\text{ic}} - \sum_{j \in \text{CU}} Q_{p,i,j}^{\text{ex}}) - \sum_{j \in \text{STR}'} \Delta Q_{p,j}^{\text{ir}} \quad (8)$$

$$Q_p^{\text{rb}} = Q_{0,p}^{\text{rb}} - \sum_{j \in \text{STR}'} \left( \sum_{i \in \text{HU}} Q_{p,i,j}^{\text{ex}} - \Delta Q_{p,j}^{\text{ir}} \right) - \sum_{i \in \text{REC}'} \Delta Q_{p,i}^{\text{ic}} \quad (9)$$

where  $Q_{0,p}^{\text{cn}}$  and  $Q_{0,p}^{\text{rb}}$  are the condenser and reboiler duty before any heat exchange and  $Q_p^{\text{cn}}$  and  $Q_p^{\text{rb}}$  are those values resulted from heat exchange at stages.  $Q_{p,i,j}^{\text{ex}}$  is the heat exchanged between a heat source  $i$  and a heat sink  $j$ . REC' and STR' are the sets of stages in the rectifying section excluding the top condenser and that excluding the bottom reboiler, respectively.  $\Delta Q_{p,i}^{\text{ic}}$  and  $\Delta Q_{p,j}^{\text{ir}}$  are explicit mathematical expressions that estimate the relationships between the net reduction of the condenser and reboiler duty, and the heat removed or supplied

in an intermediate condenser or intermediate reboiler installed at stage  $i$  or  $j$  for each product  $p$ . Since  $\Delta Q_{p,i}^{ic}$  and  $\Delta Q_{p,j}^{ir}$  are indicators of the inefficiency in the condenser and reboiler duty reduction resulted from heat exchange, large values must be avoided. Section S3 in the Supporting Information shows in detail the calculation of  $\Delta Q_{p,i}^{ic}$  and  $\Delta Q_{p,j}^{ir}$  as well as the parameters to calculate  $\Delta Q_{p,i}^{ic}$  for the MTRD at 2.5 bar.

Equation 10 shows the necessary constraint to enforce feasible heat exchange, which is based on the “Big- $M$ ” formulation. It is a valid representation of linear constraints, and it generates small MILP problems<sup>20</sup>

$$Q_{p,i,j}^{ex} - M\Delta T_{p,i,j}^{ex} Y_{p,i,j}^{ex} \leq 0 \quad i \in \text{HSO}, j \in \text{HSI} \quad (10)$$

where  $M$  is a big enough value,  $\Delta T_{p,i,j}^{ex}$  is the logarithmic mean temperature difference between a heat source  $i$  and sink  $j$ , and  $Y_{p,i,j}^{ex}$  is a binary variable which becomes one if a heat exchanger is installed between a heat source  $i$  and sink  $j$ , and zero otherwise. HSO is the set of heat sources and HSI is the set of heat sinks.

The  $\Delta T_{p,i,j}^{ex}$  was calculated according to eq 11

$$\Delta T_{p,i,j}^{ex} = \begin{cases} \frac{(T_i^{\text{in}} - t_j^{\text{out}}) - (T_i^{\text{out}} - t_j^{\text{in}})}{\ln[(T_i^{\text{in}} - t_j^{\text{out}})/(T_i^{\text{out}} - t_j^{\text{in}})]}, & \text{if } T_i^{\text{in}} - t_j^{\text{out}} \geq \Delta T_{\text{min}} \text{ and } T_i^{\text{out}} - t_j^{\text{in}} \geq \Delta T_{\text{min}} \\ 0, & \text{otherwise} \end{cases} \quad (11)$$

$i \in \text{HSO}, j \in \text{HSI}$

where  $T^{\text{in}}$  and  $T^{\text{out}}$  are the inlet and outlet temperatures of the heat source  $i$  while  $t^{\text{in}}$  and  $t^{\text{out}}$  are the inlet and the outlet temperatures of the heat sink  $j$ ,  $\Delta T_{\text{min}}$  is the allowed minimum temperature difference.

Through the discretization of the cooling temperature in the refrigeration cycles ( $t_{s,i,r}^{\text{out}}$ ) and refrigeration cost ( $C_r^{\text{ref}}$ ), and the linearization of  $\Delta Q_{p,i}^{ic}$  and  $\Delta Q_{p,j}^{ir}$ , the optimization model can be solved as a mixed integer linear programming (MILP) problem. This problem can find the best heat exchange network between heat sources and sinks, and it is solved in combination with the simulation software Aspen Plus 8.6.

Since reactive distillation is inherently characterized by a set of nonlinear and nonconvex equations, in the simulation, the bilinear terms in the mass balance, nonlinear thermodynamic relations, complex enthalpy calculations, energy balance, and complex kinetics are readily solved. Thus, by combining the strong points of optimization and simulation, the optimal solution was found.

Optimizations and simulations are iteratively combined through an interface programmed in Excel VBA, and eq 12 shows the convergence criterion. It is based on the Euclidean distance between changes in the reactive distillation column temperature profile at the  $s$ th iteration and that at the  $s+1$  iteration

$$\sqrt{\sum_{i \in \text{REC}} (T_{p,i,s} - T_{p,i,s+1})^2 + \sum_{j \in \text{STR}} (T_{p,j,s} - T_{p,j,s+1})^2} \leq N\varphi \quad (12)$$

$p \in \text{PRO}, s \in \text{IT}$

where  $N$  is the total number of stages in the RD column,  $\varphi$  is a small number (e.g., 0.001), and IT is the set of necessary iterations to achieve convergence.

For the sake of clarity, Figure S3 in the Supporting Information shows the convergence for the installation of intermediate heat exchangers in an RD that produces silane at 2.5 bar.

Figure 4 shows the solution procedure that combines the simulation software Aspen Plus V.8.6 and the optimization

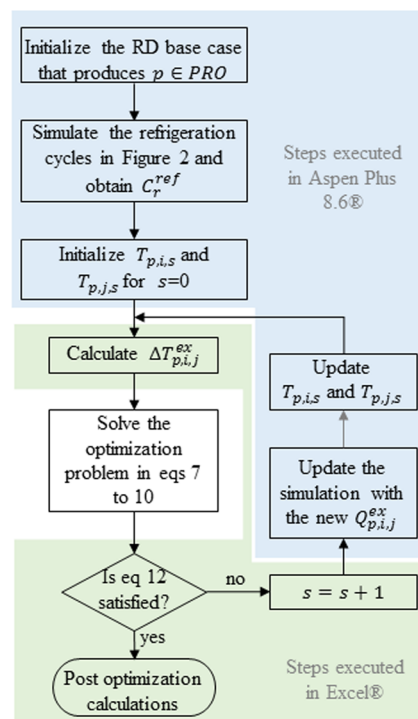


Figure 4. Solution procedure.

software IBM ILOG CPLEX Optimization Studio 12.5. The procedure in the figure is repeated three times, one per product (S, MCS, and DCS).

The solution procedure is described as follows:

1. Take a base case RD without any intermediate heat exchanger.
2. Simulate the refrigeration cycles and calculate  $C_j^{\text{cool}}$  for each one.
3. Initialize all the remaining necessary parameters in the optimization problem and set  $T_{p,i,s}$  and  $T_{p,j,s}$  for  $s = 0$ .
4. Calculate  $\Delta T_{p,i,j}^{ex}$  in the Excel interface and solve the MILP problem.
5. Exit the procedure if the convergence criterion is met and execute the post optimization calculations. If not, go to step 6.
6. Export the optimization results to the interface and from the interface to the simulation.
7. Execute the simulation for the new values of  $Q_{p,i,j}^{ex}$  and set  $s = s + 1$ .
8. Export the simulation results to the interface and update  $T_{p,i,s}$  and  $T_{p,j,s}$ .
9. Repeat steps 4 to 8 until satisfying the convergence criterion in eq 12.

**4.2. Post-optimization Cost Evaluation.** Because changes in the structural variables cannot be made once the process is designed, this section explains the criteria to select the size of the distillation column, trays, and heat exchangers. Equation 13 shows the calculation of the equipment cost (EC)

$$EC = C^{\text{vess}} + C^{\text{tray}} + \sum_{i \in \text{REC}} C_i^{\text{ex}} + \sum_{j \in \text{STR}} C_j^{\text{ex}} \quad (13)$$

where  $C^{\text{vess}}$  is the cost of the column vessel,  $C^{\text{tray}}$  is the cost of the trays, and  $C^{\text{ex}}$  is the cost of heat exchangers either in the rectifying and stripping section.

$C^{\text{vess}}$  and  $C^{\text{tray}}$  are functions of the column diameter, which depends on the flooding ratio, vapor flow rate, and liquid holdup. Equations 14 and 15 show the calculations of  $C^{\text{vess}}$  and  $C^{\text{tray}}$ , respectively,

$$C^{\text{vess}} = \max_{p \in \text{PRO}} \{C_p^{\text{vess}}(D_i)\} \quad (14)$$

$$C^{\text{tray}} = N(\max_{p \in \text{PRO}} \{C_p^{\text{tray}}(D_i)\}) \quad (15)$$

where  $C_p^{\text{vess}}$  and  $C_p^{\text{tray}}$  are the vessel and tray costs of each RD column that produces  $p$ .  $D_i$  is the internal diameter of the RD column.

Since the columns that produce S, MCS, and DCS are individually designed and optimized, there are three values of  $C_p^{\text{vess}}$  and  $C_p^{\text{tray}}$ . If the column with the smallest diameter is selected, it might be difficult, if not impossible, to reach the internal liquid and vapor flow rates for the production of other components without suffering from flooding. Contrarily, if the column with the largest diameter is selected, the equipment will have the flexibility to shift the internal liquid and vapor flow rates; however, it is important to carefully set this diameter to avoid weeping or dumping.

$C_i^{\text{ex}}$  and  $C_j^{\text{ex}}$  are functions of the heat exchanger area, which depends on the amount of heat transferred, temperature difference between cooling and heating fluids and the overall heat transfer coefficient. Equations 16 and 17 show the calculations of  $C_i^{\text{ex}}$  and  $C_j^{\text{ex}}$ , respectively,

$$C_i^{\text{ex}} = \sum_{j \in \text{CU}} \max_{p \in \text{PRO}} \{C_{p,i,j}^{\text{ex}}(A_{p,i,j}^{\text{ex}})\} \quad (16)$$

$$C_j^{\text{ex}} = \sum_{i \in \text{HU}} \max_{p \in \text{PRO}} \{C_{p,i,j}^{\text{ex}}(A_{p,i,j}^{\text{ex}})\} \quad (17)$$

where  $C_{p,i,j}^{\text{ex}}$  is the cost and  $A_{p,i,j}^{\text{ex}}$  is the heat transfer area of a heat exchanger that is installed between a heat source  $i$  and a heat sink  $j$  for each product  $p$ .

Equation 18 shows the relation between the heat transfer area and the amount of exchanged heat

$$A_{p,i,j}^{\text{ex}} = \frac{Q_{p,i,j}^{\text{ex}}}{U(\Delta T_{p,i,j}^{\text{ex}} + \varphi)} \quad p \in \text{PRO}, i \in \text{HSO}, j \in \text{HSI} \quad (18)$$

where  $U$  is the overall heat transfer coefficient, and  $\varphi$  is a small number to avoid division by zero for infeasible heat exchanges.

For  $C_i^{\text{ex}}$ , there are three times the number of stages in the rectifying section for each cooling utility while for  $C_j^{\text{ex}}$ , there are three times the number of stages in the stripping section for each heating utility. Moreover, if different cooling utilities for different products exchange heat at the same stage in the rectifying section, two heat exchangers are installed. However, if the same cooling utility in different products exchanges energy at the same stage in the rectifying section, only one heat exchanger, the largest, is installed.

The cost calculations in this work were done according to the method reported in Seider et al.<sup>21</sup> Carbon steel was the assumed equipment material. However, if different construction

materials were assumed, different heat exchangers would be installed at the same stage even for the same cooling utility.

Equation 19 shows the total annual cost (TAC) calculation of the MTRD

$$\text{TAC} = \frac{EC}{\text{PB}} + \text{OC} \quad (19)$$

where PB is the payback time of the process.

Table S9 in the Supporting Information exemplifies how the equipment cost was calculated in the RD that produced S, MCS, and DCS at 2.5 bar.

## 5. RESULTS AND DISCUSSION

The solution procedure to design a multitask reactive distillation column with intermediate heat exchangers is applied for the cases in Table 5. Cases 1 and 2 show an equal

**Table 5. Evaluated Cases To Design an MTRD with Intermediate Heat Exchangers**

	$\theta_s/\theta_i/\theta_s$ [h]	column pressure
case 1 (C1)	2833/2833/2833	same pressure for all products
case 2 (C2)		variable pressure for all products
case 3 (C3)	6800/850/850	same pressure for all products
case 4 (C4)		variable pressure for all products

distribution in the production of silane, monochlorosilane, and dichlorosilane while cases 3 and 4 show a distribution with much more production of silane over monochlorosilane and dichlorosilane.

From the reaction performance viewpoint, the reaction in eq 3 is exothermic and those in eqs 1 and 2 are slightly endothermic. For reversible endothermic reactions, an increase in pressure improves the conversion and speeds up the reaction rate if the reaction is equimolar because a pressure increase corresponds to a temperature increase. From the separation performance viewpoint, an increase in pressure results in an increase of the boiling point of the components and a decrease in their relative volatility. Therefore, the separation becomes more difficult.

The RD columns were simulated in a range of several pressures to consider the maximum catalyst operating temperature, and reaction and separation performances. The simulated pressure range was taken from Ramírez-Márquez et al.<sup>13</sup> They found a range between 2 and 2.33 bar with a good trade-off between cost and column top pressure.

In cases 1 and 3, the MTRD column operates at the same pressure, thus the production of S, MCS, and DCS shifts by changing the vapor and liquid internal flow rates. In cases 2 and 4, the MTRD column can operate at a different pressure in addition to the changes in vapor and liquid internal flow rates.

Table 6. shows the additional parameters that were used in the solution procedure in section 4.

**Table 6. Additional Parameters**

parameter	value
M [-]	50
MS (steam at 6.2 bar) [\$/kWh]	0.0506
$U$ [kW/m <sup>2</sup> K]	0.5
PB [yr]	10
$\Delta T_{\text{min}}$ [K]	10

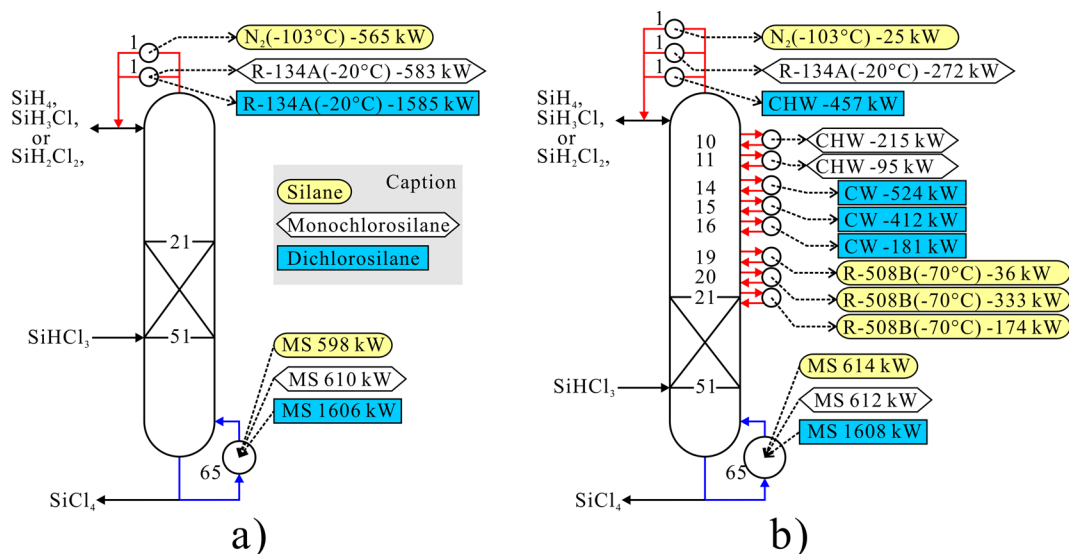


Figure 5. MTRD at 2.5: (a) conventional and (b) optimized.

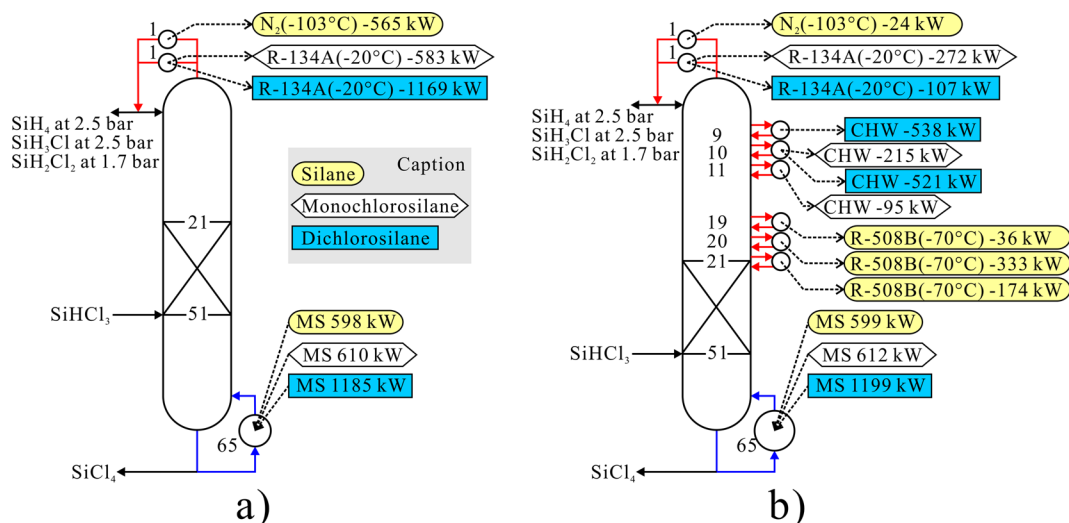


Figure 6. MTRD at variable pressure: (a) conventional and (b) optimized.

Figure 5 shows the results at 2.5 bar for the conventional MTRD and the optimized MTRD with intermediate condensers. The conventional MTRD does not have any intermediate condenser, but the optimized one has eight intermediate condensers in total. For silane, the intermediate condensers are located between stages 19 and 21. For monochlorosilane, the intermediate condensers are located at stages 10 and 11. Finally, for dichlorosilane, the intermediate condensers are located between stages 14 and 16. Although the optimized MTRD has installed eight intermediate condensers, it uses a maximum of three intermediate condensers at a time. It can be seen that the refrigerant R-134A was substituted by CHW, which is cheaper because the temperature difference for CHW is smaller than that for R-134A. Thus, the use of CHW is only advantageous when a small amount of heat is exchanged. Contrarily, when a high amount of heat is exchanged, the necessary heat exchanger area is large, which results in an expensive heat exchanger. In this sense, R-134A is only advantageous when a large amount of heat is exchanged. Figures S4 to S8 in the Supporting Information show in detail the results for the optimal solutions at 1.7, 2.1, and 2.5 bar.

Figure 6 shows the results for the conventional MTRD and the optimized MTRD with intermediate condensers when the pressure is variable. The conventional MTRD does not have any intermediate condenser, but the optimized one has seven intermediate condensers in total. For the production of silane and monochlorosilane, the column operates at 2.5 bar while for dichlorosilane it operates at 1.7 bar. For silane three intermediate condensers are located between stages 19 and 21, for monochlorosilane the intermediate condensers are located at stages 10 and 11, and for dichlorosilane, the intermediate condensers are located at stages 9 and 10. Although the optimized MTRD has installed seven intermediate condensers, it uses a maximum of three intermediate condensers at a time.

When silane is produced, the best operating pressure is 2.5 bar because at this condition, a less expensive refrigerant ( $N_2$  at  $-103^\circ C$ ) is used in comparison with the operation at 1.7 and 2.1 bar, which uses  $N_2$  at  $-112^\circ C$ . When monochlorosilane is produced, the best operating pressure is also 2.5 bar because at this condition, the refrigerant R-134A at  $-20^\circ C$  is used because the heat transfer area is smaller in comparison with the

Table 7. TAC Results (k\$/yr) for Cases 1 and 2<sup>a</sup>

	case 1						case 2	
	1.7 bar		2.1 bar		2.5 bar		variable pressure	
	c-MTRD	o-MTRD	c-MTRD	o-MTRD	c-MTRD	o-MTRD	c-MTRD	o-MTRD
$C^{\text{vess}} + C^{\text{tray}}$	339	339	352	352	365	365	365	365
$\sum_{i \in \text{REC}} C_i^{\text{ex}} + \sum_{j \in \text{STR}} C_j^{\text{ex}}$	279	383	277	464	234	438	207	296
EC	618	722	629	816	599	803	571	661
heating	457	457	463	467	402	403	343	343
cooling	4254	1015	3468	1421	2789	346	2732	383
TAC	4773	1544	3998	1966	3253	828	3132	792
reduction rate [%]		68		51		75		75

<sup>a</sup>Notation: c-MTRD, conventional MTRD; o-MTRD, optimized MTRD.

Table 8. TAC Results (k\$/yr) for Cases 3 and 4

	case 3						case 4	
	1.7 bar		2.1 bar		2.5 bar		variable pressure	
	c-MTRD	o-MTRD	c-MTRD	o-MTRD	c-MTRD	o-MTRD	c-MTRD	o-MTRD
$C^{\text{vess}} + C^{\text{tray}}$	339	339	352	352	365	365	365	365
$\sum_{i \in \text{REC}} C_i^{\text{ex}} + \sum_{j \in \text{STR}} C_j^{\text{ex}}$	279	383	277	464	234	438	207	296
EC	618	722	629	816	599	803	571	661
heating	394	396	344	344	301	301	283	284
cooling	9217	1960	7258	3028	6067	669	6,050	680
TAC	9673	2428	7664	3454	6428	1050	6390	1029
reduction rate [%]		75		55		84		84

Table 9. Gap Optimality between Optimal and Suboptimal Solutions

	case 1 at 2.5 bar			case 2		
	suboptimal solutions			suboptimal solutions		
	(3/3/3) <sup>a</sup>	(2/2/2)	(1/1/1)	(3/3/3) <sup>a</sup>	(2/2/2)	(1/1/1)
no. of intermediate heat exchangers (SiH <sub>4</sub> / SiH <sub>3</sub> Cl/SiH <sub>2</sub> Cl <sub>2</sub> )						
				cost [k\$/yr]		
$C^{\text{vess}} + C^{\text{tray}}$	<b>365</b>	365	365	<b>365</b>	365	365
$\sum_{i \in \text{REC}} C_i^{\text{ex}} + \sum_{j \in \text{STR}} C_j^{\text{ex}}$	<b>420</b>	412	440	<b>363</b>	356	384
EC	<b>785</b>	777	805	<b>728</b>	721	749
heating	<b>469</b>	455	431	<b>404</b>	391	368
cooling	<b>811</b>	885	1,514	<b>864</b>	933	1,578
TAC	<b>1359</b>	1418	2026	<b>1341</b>	1396	2021
relative gap with optimal solutions [%]	<b>64.1</b>	71.3	144.7	<b>69.3</b>	76.3	155.2

<sup>a</sup>A unique set of three intermediate heat exchangers is installed for all products. The solutions in bold correspond to the case when a single set of three heat exchangers is used for the three products (stages 19 to 21 for Cases 1 and 2).

operation at 1.7 and 2.1 bar. When dichlorosilane is produced, the best operating pressure is 1.7 bar because, at this condition, the amount of CHW and steam is less in comparison with the operation at 2.1 and 2.5 bar.

Table 7 summarizes the results for cases 1 and 2. As the column pressure increases, its temperature profile also increases. From the reaction viewpoint, the reaction system shifts toward the products, which causes an adverse condition. From the separation aspect, the pressure increase is also undesirable because the separation becomes more difficult as the relative volatility decreases. Nevertheless, in case 1 from the economic aspect, an increase of pressure and temperature is favorable because the column needs less expensive refrigerants or uses water as a cooling medium.

In case 1 the columns at 2.1 and 2.5 bar have eight intermediate condensers (i.e., three for SiH<sub>4</sub> production, two for SiH<sub>3</sub>Cl production, three for SiH<sub>2</sub>Cl<sub>2</sub> production). However, the column at 2.1 bar is more expensive because the temperature difference is smaller between the column

stages and the refrigeration cycles. The cost of the six intermediate condensers for the column at 1.7 is the smallest (i.e., two for the production of each component); however, for the production of monochlorosilane at 1.7 bar, the refrigerant R-407D is used, which is more expensive than the chilled water used at the condenser in the column at 2.5 bar. Therefore, when the operating pressure of the column is the same, the column at 2.5 bar is the best option.

In case 2, silane and monochlorosilane use more expensive refrigerants at 1.7 and 2.1 bar (N<sub>2</sub> at -112 °C and R-407D at -30 °C, respectively, in Figures S4 to S7 in the Supporting Information) than those at 2.5 bar. Since refrigerants are not needed for the production of dichlorosilane, the column at 1.7 bar represents the best option because lower operating pressure is favorable to perform the separation. Therefore, from the economic viewpoint, the MTRD column has the minimum cost when the column operates at 2.5 bar for the production of silane and monochlorosilane, and at 1.7 bar for the manufacture of dichlorosilane.

The optimal solutions for case 1 and case 2 in Figure 6 are the same for case 3 and case 4, respectively, but the TAC is different in each case. Because the cost of the MTRD column is mostly dominated by the operating cost when silane is produced, an increase in the demand of silane will increase the potential economic savings of the MTRD column. Table 8 summarizes the results for cases 3 and 4.

Intuitively, the installation of fewer intermediate heat exchangers can ease and simplify the process control. Table 9 shows the gap optimality between the optimized MTRD in Figures 5b and 6b and some suboptimal solutions with fewer intermediate heat exchangers.

Although these solutions use fewer heat exchangers, their equipment and heating cost are the highest because the locations of intermediate heat exchangers are far from the column top, which results in large values of  $\Delta Q_{p,i}^{ic}$ . The previous situation implies more heating and a larger bottom reboiler.

The selection of a unique set of intermediate heat exchangers for all products results in an MTRD with an expected control easier and TAC lower than the suboptimal solutions in Table 9. However, the optimal solutions in Figures 5b and 6b, which have different sets of intermediate heat exchangers for each product, attain the lowest TAC. If there is not flexibility in choosing the best location of each intermediate heat exchanger for every different product, the TAC will increase. Therefore, it is economically better to have a design with flexible locations of intermediate heat exchangers. The solutions with a unique set of intermediate heat exchangers are 64.1% and 69.3% more expensive than the optimized MTRD with flexible intermediate heat exchangers.

Table 10 shows the results when three independent columns with intermediate heat exchangers are installed. The locations

**Table 10. Cost Estimation (k\$/yr) of Cases 2 and 4 When Three Independent Columns Are Used<sup>a</sup>**

	silane	monochlorosilane	dichlorosilane
$C^{\text{vess}} + C^{\text{tray}}$	295	329	365
$\sum_{i \in \text{REC}} C_i^{\text{ex}} + \sum_{j \in \text{STR}} C_j^{\text{ex}}$	112	160	207
EC	407	489	572
heating	86 (206)	88 (26)	169 (51)
cooling	269 (645)	52 (16)	63 (19)
TAC [k\$/yr]	396 (892)	189 (91)	289 (127)
overall TAC [k\$/yr]	874 (1110)		

<sup>a</sup>The results in parentheses correspond to Case 4.

of the heat exchangers correspond to the ones in Figure 6b. As it can be seen, the TAC of the single flexible column in Figure 6b (i.e., 792 and 1029 k\$/yr for cases 2 and 4, respectively) is smaller than the installation of three columns (i.e., 874 and 1110 k\$/yr for cases 2 and 4, respectively) because more equipment is installed. The equipment cost is the same in cases 2 and 4, only the operation cost is different.

**5.1. Post-optimization Validation of Results.** The reported solutions in Figures 5 and 6 were obtained from executing the solution procedure in Figure 4. In the solution procedure, actual intermediate heat exchangers are not installed, but the effect of heat exchange is considered by using the feature “heaters and coolers” in the RadFrac module of Aspen Plus 8.6. The comparison between the proposed method and the rigorous simulations that include in detail the installation of heat exchangers is made to validate the reliability

of the proposed solution procedure. Section S7 in the Supporting Information shows the comparison of these results.

## 6. CONCLUSIONS

In this work a multitask reactive distillation (MTRD) column that produces silane, monochlorosilane, and dichlorosilane is designed through a proposed solution procedure in which rigorous simulations and optimizations are combined and executed iteratively. Four case studies were done to evaluate two production demands and to assess the effect of changing the operating pressure in the column. Since silane has a very low boiling point ( $-112.15$  °C at 1.01 bar), refrigeration cycles were also designed to supply cooling at several discrete temperatures. When the pressure remains constant in the column, high-pressure operation (2.5 bar) was the best solution because less expensive cooling utilities are available. Contrarily, when the pressure can change between products, high-pressure operation (2.5 bar) for silane and monochlorosilane and low-pressure operation (1.7 bar) for dichlorosilane was the best solution because less expensive utility and less utility demand are used. The optimal MTRD columns are better than designs of three independent reactive distillation columns and MTRD columns with a unique set of few intermediate heat exchangers. Rigorous and detailed simulations were done to validate the reliability of the proposed solution procedure, and the comparison results showed good agreement between the derived solutions from the proposed procedure.

## ■ ASSOCIATED CONTENT

### 📄 Supporting Information

The Supporting Information is available free of charge on the ACS Publications website at DOI: 10.1021/acs.iecr.6b02277.

Design of the reactive distillation columns optimized independently and the conventional design of the MTRD; design of refrigeration cycles; calculations of the delta terms in eqs 7 and 8; cost equipment functions; post-optimization results; additional optimization results of suboptimal solutions; validation results in Aspen Plus 8.6 (PDF)

## ■ AUTHOR INFORMATION

### Corresponding Author

\*E-mail: jrafael.alcantara@tokushima-u.ac.jp. Tel.: +81-88-656-7425.

### Notes

The authors declare no competing financial interest.

## ■ REFERENCES

- Bye, G.; Ceccaroli, B. Solar grade silicon: Technology status and industrial trends. *Sol. Energy Mater. Sol. Cells* **2014**, *130*, 634–646.
- Andrews, R. N.; Clarkson, S. J. Pathways to solar grade silicon. *Silicon* **2015**, *7* (3), 303–305.
- Agarwal, A. K.; Lehmann, J. F.; Coe, C. G.; Temple, D. J. *Method for making a chlorosilane*. U.S. Patent 8,206,676 B2, Jun 26, 2012.
- Zhu, M.; Lerum, M. Z.; Chen, W. How to prepare reproducible, homogeneous, and hydrolytically stable aminosilane-derived layers on silica. *Langmuir* **2012**, *28* (1), 416–423.
- Bagatur'yants, A. A.; Novoselov, K. P.; Safonov, A. A.; Cole, J. V.; Stoker, M.; Korin, A. A. Silicon nitride chemical vapor deposition from dichlorosilane and ammonia: theoretical study of surface structures and reaction mechanism. *Surf. Sci.* **2001**, *486* (3), 213–225.
- Breneman, W. C. High purity silane and silicon production. U.S. Patent 4,676,967, Jun 30, 1987.

(7) Huang, X.; Ding, W. J.; Yan, J. M.; Xiao, W. D. Reactive distillation column for disproportionation of trichlorosilane to silane: reducing refrigeration load with intermediate condensers. *Ind. Eng. Chem. Res.* **2013**, *52* (18), 6211–6220.

(8) Alcántara-Avila, J. R.; Sillas-Delgado, H. A.; Segovia-Hernández, J. G.; Gómez-Castro, F. I.; Cervantes-Jauregui, J. A. Optimization of a reactive distillation process with intermediate condensers for silane production. *Comput. Chem. Eng.* **2015**, *78* (12), 85–93.

(9) Breneman, W. C. Process for production of silane and hydrohalosilanes. U.S. Patent 0,156,675 A1, Jun 20, 2013.

(10) Wajge, R. M.; Reklaitis, G. V. An Optimal campaign structure for multicomponent batch distillation with reversible reaction. *Ind. Eng. Chem. Res.* **1998**, *37* (5), 1910–1916.

(11) Kapilakam, K.; Luyben, W. L. Plantwide control of continuous multiproduct processes: three-product process. *Ind. Eng. Chem. Res.* **2003**, *42* (12), 2809–2825.

(12) Tseng, Y.-T.; Ward, J. D.; Lee, H.-Y. Design and control of a continuous multi-product process with product distribution switching: sustainable manufacture of furfuryl alcohol and 2-methylfuran. *Chem. Eng. Process.* **2016**, *105*, 10–20.

(13) Ramírez-Márquez, C.; Sánchez-Ramírez, E.; Quiroz-Ramírez, J. J.; Gómez-Castro, F. I.; Ramírez-Corona, N.; Cervantes-Jauregui, J. A.; Segovia-Hernández, J. G. Dynamic Behavior of a Multi-Tasking Reactive Distillation Column for Production of Silane, Dichlorosilane and Monochlorosilane. *Chem. Eng. Process.* **2016**, *108*, 125.

(14) Noeres, C.; Kenig, E. Y.; Górak, A. Modelling of reactive separation processes: reactive absorption and reactive distillation. *Chem. Eng. Process.* **2003**, *42*, 157–178.

(15) Keller, T.; Dreisewerd, B.; Górak, A. Reactive distillation for multiple-reaction systems: optimization study using an evolutionary algorithm. *Chem. Process Eng.* **2013**, *34* (1), 17–38.

(16) Luyben, W. L.; Yu, C.-C. *Reactive Distillation Design and Control*; John Wiley & Sons, Inc.: Hoboken, NJ, 2008; pp 17–36.

(17) Product data Sheet Amberlyst A21. <http://www.hopegood.biz/upload/12744365841352.pdf> (accessed May 12, 2016).

(18) Turney, M. A.; Briglia, A. Method for improved thermal performing refrigeration cycle. U.S. Patent US20140157824 A1, Jun 12, 2014.

(19) Ministry of Economy, Trade and Industry. Standard of electricity prices (in Japanese). [http://www.meti.go.jp/committee/sougouenergy/denryoku\\_gas/kihonseisaku/pdf/002\\_04\\_02.pdf](http://www.meti.go.jp/committee/sougouenergy/denryoku_gas/kihonseisaku/pdf/002_04_02.pdf) (accessed Aug 29, 2016).

(20) Trespalacios, F.; Grossmann, I. E. Improved Big-M reformulation for generalized disjunctive programs. *Comput. Chem. Eng.* **2015**, *76*, 98–103.

(21) Seider, W. D.; Seader, J. D.; Lewin, D. R.; Widagdo, S. *Product and Process Design Principles*, International Student Version; Wiley, 2010; pp 557–595.